ICNTC-2019 Special Issue

J. Indian Chem. Soc.,
Vol. 96, September 2019, pp. 1123-1130

Structural and electronic properties of layered semiconductor chalcogenide crystals: $TlGaSe_2$, $TlGaS_2$ and $TlInS_2$

Burak Gurkan and Savas Berber*

Department of Physics, Gebze Technical University, Gebze-Kocaeli, Turkey

E-mail: savasberber@gtu.edu.tr

Manuscript received online 26 April 2019, revised and accepted 20 July 2019

We report the density functional theory structure optimization and electronic structure calculations of $TlGaSe_2$, $TlGaS_2$, and $TlInS_2$ compounds. We find that there is a weak bonding between Tl and the chalcogen while Ga and In make covalent bonds with the chalcogen. The s orbitals of the chalcogen hybridize with the d orbitals of Tl, bringing additional directionality to the Tl-chalcogen interaction. There is no direct Tl-Tl bond. Although these three compounds are extremely similar, the band structures exhibit quantitative and qualitative differences. The optimized $TlGaSe_2$ and $TlInS_2$ crystals have direct band gaps while $TlGaS_2$ has an indirect gap. The lowest unoccupied states have a bonding character between the p orbitals of the adjacent Tl atoms. These states form conduction channels along the Tl chains. The valence band maximum originates from Tl-s orbitals and its position in the Brillouin zone is robust. Almost degenerate Tl-p related bands are affected differently by the interlayer interaction. Therefore, minute changes in the structure may shuffle their energy levels, resulting in qualitatively and quantitatively different band gaps in these extremely similar compounds. External pressure and defects may initiate the same type of electronic structure changes resulting in contradicting results in experiments. A small down-shifting of the unoccupied parabolic bands lead to several valleys in the conduction band of $TlGaSe_2$.

Keywords: Semiconductor chalcogenides, layered crystal, electronic structure.

Introduction

The ternary semiconductors $TlGaSe_2$, $TlGaS_2$, and $TlInS_2$ are in the family of monoclinic $A_3B_3C_2^6$ chalcogenide crystals[1,2]. They are layered structures with anisotropic properties[3,4]. These compounds show several phase transitions at low temperatures[5–7] or under high pressure[8,9]. Along with the phase transitions, the electronic and optical properties are modified[8,10,11], indicating a delicate relationship between the structure and the electronic structure[12]. Small changes in the structure are linked to the optical and electronic properties[13,14]. These materials have a potential to find new applications[15–17] that could take advantage of their layered structure.

Understanding the physical phenomena in these Tl-based ternary systems requires a detailed investigation of the electronic structure and the bonding, which was the subject of illuminating early works[18,19]. The positions of Tl atoms were suggested to be the source of the observed phase transitions[19] on the basis of tight-binding calculations on suitable models. Density functional theory calculations for the electronic structure using linear muffin-tin orbital (LMTO) method[20], linearized augmented plane wave (LAPW) method[21], and local-density approximation (LDA) were reported[22,23]. These related works cannot agree on the character of the band gaps and the position of the conduction band minimum. In a recent study[24], the experiments indicate a direct gap for $TlGaSe_2$ while the computational part of the same work shows an indirect band gap. These Tl-based ternary semiconductors are far from being perfect[24,25]. We believe the diverse results in the literature[3] are somehow related to the delicate relationship between the structure and the electronic structure.

In this work, we aim to find the causes of the close relationship between the structure and the electronic structure. We did through structure optimizations and compared the electronic band structures. The three compounds are extremely similar but show different physical phenomena. The causes of the differences in their electronic structures are

discussed in the following while demonstrating their striking similarities.

Computational

We carried out structure optimization and electronic structure calculations in the density functional theory (DFT)[26] within generalized gradient approximation (GGA). The exchange-correlation interaction was described by Perdew-Burke-Ernzerhof (PBE) functional[27]. We obtained lattice vectors along with the relaxed atom coordinates. Initial atom coordinates and lattice vectors were taken from crystallographic data[1,2]. The electronic structures were calculated before and after the structure optimizations. This was to pinpoint the causes of varying reports in the literature. We used norm-conserving Troullier-Martins pseudo-potentials[28] with non-linear core corrections[29] to handle the interaction between the valence electrons and the core. The pseudo-potentials of Tl, In and Ga included d electrons in the valence. For comparison, calculations with ultrasoft pseudo-potentials[30] were also performed and consistent results were obtained. The wavefunctions were expanded into a plane-wave basis that correspond to the cutoff energy of 50 Ry. The Brillouin zone was sampled by 3×3×2 k-point sampling during structure optimizations. The band structures were calculated at 441 k-points along a path going through the high symmetry k-points of the Brillouin zone. The band plots shown in this paper are composed of only the points, and no estimation is involved in how the band lines continue.

Results and discussion

$TlGaSe_2$, $TlGaS_2$ and $TlInS_2$ chalcogenides are ternary layered compounds. They crystallize in the base-centered monoclinic system with C2/c space group and share the same basic structure shown in Fig. 1, where a tetrahedron model and a ball-and-stick model are depicted. Each tetrahedron consists of an MX_4 unit, where M = Ga or In and X = S or Se. In the unit cell, 4 tetrahedra are linked by the corner chalcogen atoms and form a larger tetrahedron of M_4X_{10}. The M_4X_{10} units in successive layers are rotated by 90° with respect to each other. The interstitial voids are filled by weakly bonding Tl^{+1} ions. There are Tl-chains along both a and b axes.

The primitive unit cell contains 16 atoms while the conventional cell has 32 atoms. A ball-and-stick model of the conventional unit cell is shown in Fig. 1(b), where only strong covalent bonds between M (Ga, In) and the chalcogen (S, Se) atoms are depicted. Close inspection of the charge density reveals that each Tl atom makes 6 bonds with the nearest chalcogen atoms. Four nearest chalcogen atoms are in the same layer, and two others are in the adjacent layer. Therefore, the interlayer interaction is due to the Tl-chalcogen bonds, which are much weaker than interlayer M-X bonds. However, this interlayer bonding should not be confused with dispersion forces. These compounds are regarded as layered materials since the bonding is anisotropic.

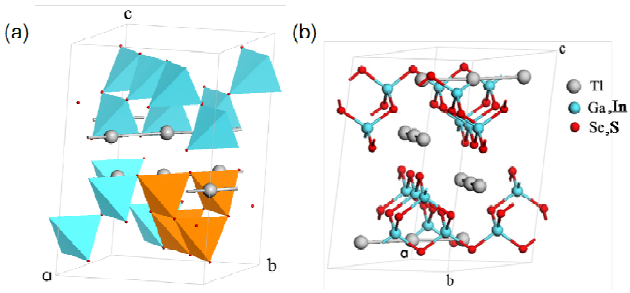

Fig. 1. The common structure of $TlGaSe_2$, $TlGaS_2$ and $TlInS_2$ chalcogenides as (a) tetrahedron and (b) ball-and-stick models.

The positions of Tl^{+1} ions are determined by their bonding to the nearest chalcogen X atoms. The Tl-X bonds mainly originate from Tl-s and chalcogen p orbitals. However, the mixing between Tl-s and Tl-p orbitals makes the Tl-X bond directional. In our pseudo-potential calculations, we observed that it is crucial to include Tl-d orbitals in the valence. Although not as important, the inclusion of Ga-d and In-d orbitals improves the calculated results. We believe the d-orbitals are decisive in providing directionality to the Tl-chalcogen bonds, which stabilize these crystals. Although the Tl atoms form chains, the charge density indicates that there are no direct Tl-Tl bonds. There is only an indirect interaction between adjacent Tl atoms through the linking chalcogen atoms.

Since there are several notations for the high-symmetry k-points, the Brillouin zone and the high symmetry k-points are depicted in Fig. 2. In the literature, there are several choices for the path along which the band structure is calculated. Following the full path, shown in Fig. 2, we go through all the special k-points because these systems have multiple valleys in the conduction band. The same k-point labels and path are used for the three compounds investigated here. Note that the V-Γ, Y-E, and L-A lines are along the c-axis.

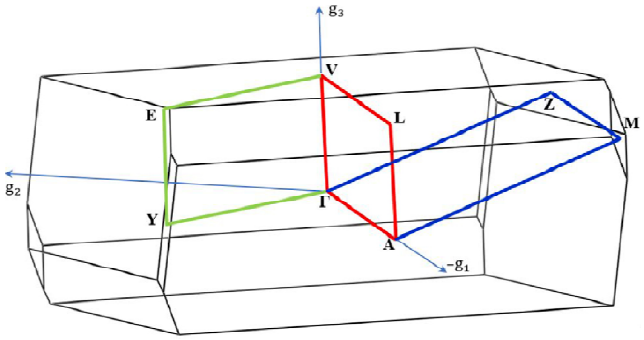

Fig. 2. The Brillouin zone of monoclinic ternary Tl-chalcogenide crystals. The high-symmetry k-points are Γ (0, 0, 0), A (–0.5, 0, 0), Z (0, –0.5, 0.5), M (–0.5, –0.5, 0.5), L (–0.5, 0, 0.5), V (0, 0, 0.5), Y (–0.5, 0.5, 0) and E (–0.5, 0.5, 0.5).

$TlGaSe_2$:

Starting from the available crystallographic data, we have optimized the lattice constants and the atom positions of $TlGaSe_2$ chalcogenide crystal. The calculated lattice parameters of the conventional cell a = 10.899 Å, b = 10.894 Å, c = 15.967 Å, and β = 99.651° are very close to the reported experimental values[2]. In the optimized structure, the Tl-Tl distance is ≈3.9 Å, and the Tl-Tl-Tl angle is ≈158°. The Tl atoms do not stay in a straight line but form a slight zigzag in the optimized structure. The Ga-Se bond length is ≈2.45 Å, and the Tl-Se distance is ≈3.23 Å on the average.

The electronic band structure of the optimized structure in Fig. 3 shows a direct band gap of 1.5 eV although the conduction band has multiple valleys that have very similar minimum values. Our calculated band gap value is smaller than the experimental values of $E_g^d \approx 2.1$ eV, $E_g^i \approx 1.8$ eV[31,32] as GGA underestimates the band gaps. The occurrence of a direct gap is in agreement with recent experiments[15,24]. A close-up view of the band structure in Fig. 5(a) illustrates the proximity of the minimums in the conduction band.

To understand the character of the bands, we have calculated the projected electronic density of states, presented in Fig. 4. As displayed in Fig. 4(a), the unoccupied bands above E_F and the occupied levels down to E_F – 8 eV originate from s and p orbitals. The Se-p orbitals participate into both the bonding and the anti-bonding bands down to E_F – 8 eV. The Ga-s and Tl-s orbitals are involved in bonding states between E_F – 8 eV and E_F – 5 eV. The anti-bonding states between E_F – 5 eV and E_F involve the hybridization between

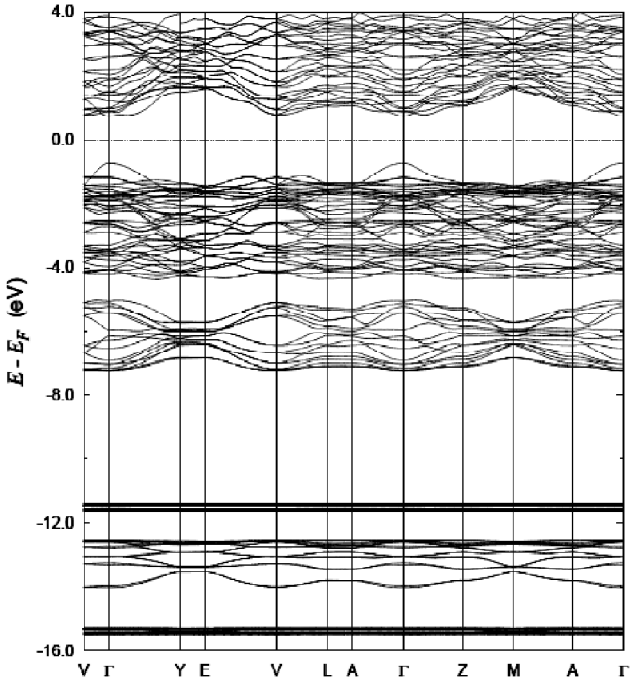

Fig. 3. Electronic band structure of $TlGaSe_2$. The energy levels are with respect to the Fermi level E_F.

Tl-s and Tl-p orbitals. The Ga-p orbitals are also present in this energy range. However, a closer look indicates that the valence band maximum (VBM) is an anti-bonding state between Tl-s and Se-p orbitals. Therefore, the highest occupied band has a considerable dispersion along the direction perpendicular to layers because the inter-layer interaction is due to Tl-Se bonds. The VBM should be sensitive to the strain along c. Since the V-Γ line is perpendicular to layers, the states of Ga-Se covalent bonds form flat bands along the V-Γ line in the band structure, displayed in Fig. 3. The bands that have a contribution from Tl orbitals acquire dispersion along the V-Γ line.

The localized Ga-d, Tl-d and Se-s states produce peaks in the projected density of states (PDOS) in Fig. 4. The shoulders near the peaks in Fig. 4 indicate that the Ga-d, Se-s and Tl-d states mix. The Se-s levels are between Ga-d and Tl-d states. Although the d-electrons are often not considered in the discussion of the bonding in these systems, the Se-s lone pair interacts with the d-electrons of the adjacent atoms. Since both Tl-d and Se-s PDOS values are high around –9 eV in Fig. 4, the Tl-d electrons interact with Se-s electrons strongly. The PDOS of Ga in the same energy indi-

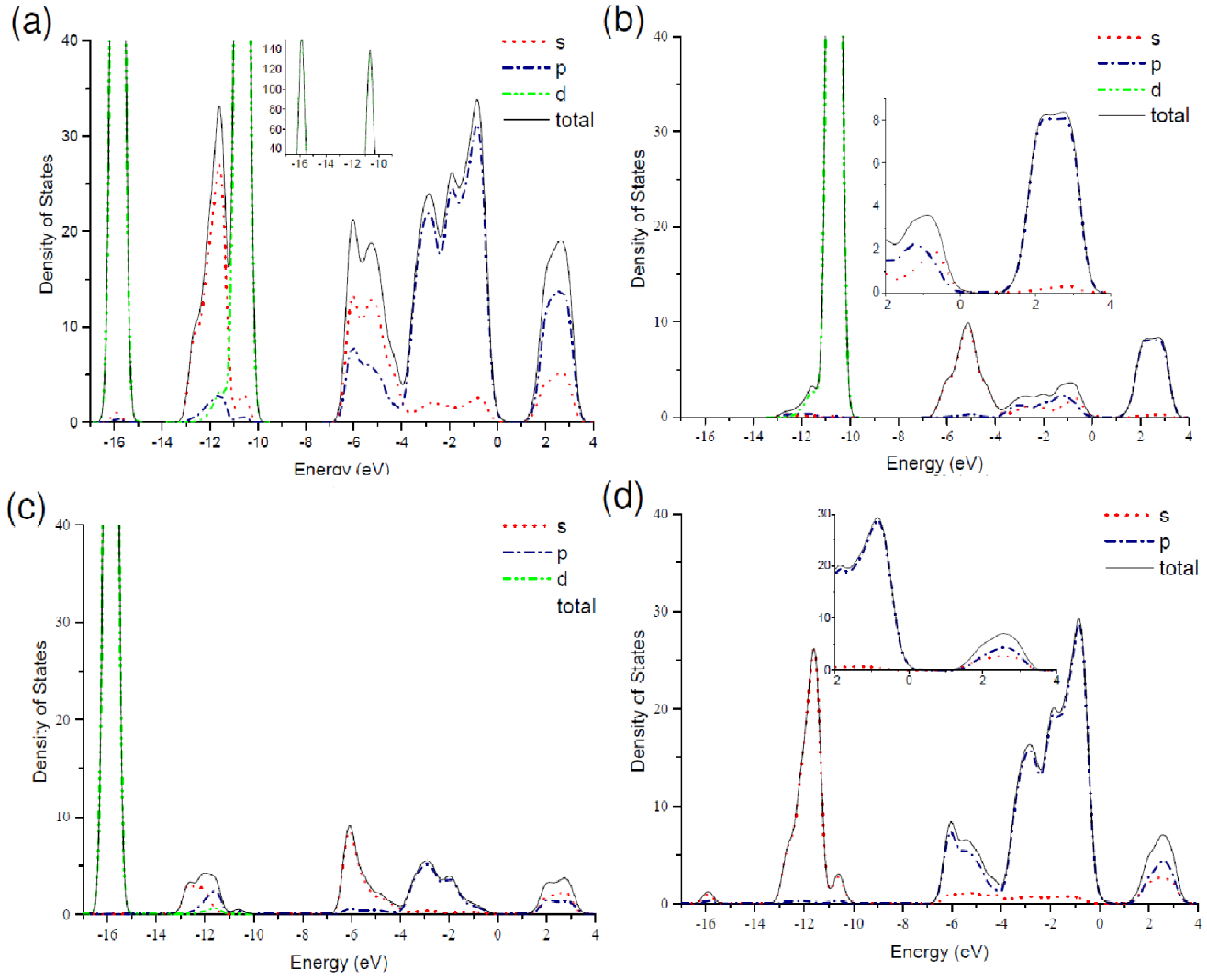

Fig. 4. (a) Electronic density of states (DOS) of $TlGaSe_2$ and projected DOS on (b) Tl, (c) Ga and (d) Se. The energy is with respect to the valence band maximum (VBM).

cates that hybridized Ga-s and Ga-p states interact with Se-s electrons while the Tl-s and Tl-p orbitals are not involved. Therefore, it was crucial to include Tl-d electrons in the valence during the calculations. We believe that the involvement of Tl-d, in addition to Tl-p, brings additional directionality to the Tl-Se bonds, crucial in stabilizing the crystal structure.

The unoccupied bands have a large contribution from Tl-p orbitals. The s and p orbitals of Ga and Se atoms are also involved with the unoccupied bands shown in Figs. 3 and 5(a). The bands that have low dispersion along the V-Γ line are in-layer states. The states that have larger dispersions along the V-Γ line include the Tl-pz orbitals that are related to the inter-layer interaction. The shape of the lowest unoccupied bands and thus the band gap heavily depends on the Tl positions because these bands are Tl-related. Therefore, the bandgap and whether it is direct or indirect correlate with minute changes in the structure, especially the position of Tl atoms. The unoptimized structure that has the Tl-Tl-Tl angle of ≈176° has an indirect band gap of 1.45 eV while the optimized structure has a direct band gap.

$TlGaS_2$:

The structure and lattice parameters of $TlGaS_2$ were optimized starting from the crystallographic data[33]. The opti-

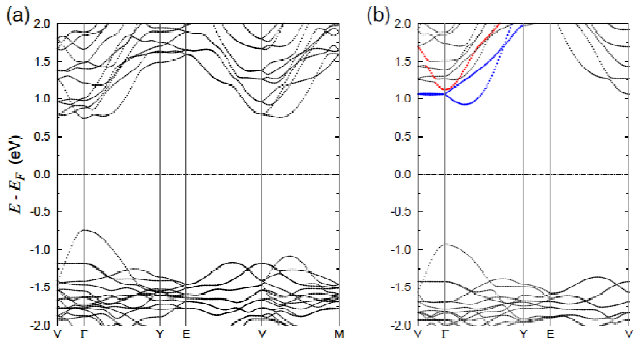

Fig. 5. Comparison of the electronic band structures of (a) $TlGaSe_2$ and (b) $TlGaS_2$.

mum lattice parameters of the conventional cell are a = 10.406 Å, b = 10.406 Å, c = 15.308 Å, and β = 99.953°. Our calculated Tl-Tl distance is ≈3.7 Å, and the Tl-Tl-Tl angle is ≈177°. Compared to $TlGaSe_2$, the Tl chains are straighter in $TlGaS_2$ with no significant deviation from the experimental values. The lattice constant of $TlGaS_2$ is smaller than $TlGaSe_2$, allowing less free play for the Tl atoms. In $TlGaSe_2$, Tl atoms get closer to some of the chalcogen neighbors while increasing the bond length to the others. Such an asymmetric bonding configuration still decreases the total energy of $TlGaSe_2$ since the occupied states contain both bonding and anti-bonding states. However, the locations of Tl in $TlGaS_2$ are tight. We find that the Ga-S bond length is ≈2.31 Å, and the Tl-S distance is ≈3.27 Å on the average.

The electronic band structure of optimized $TlGaS_2$ has the valence band maximum (CBM) at Γ point and the valence band minimum (VBM) on the Γ-Y line as shown in Fig. 6. It has an indirect band gap of 1.815 eV while the direct band gap at Γ is 1.953 eV. The unoptimized band structure had an indirect band gap of 1.768 eV even though the modifications by the structure optimization are not significant. A closer view of the band structure is displayed in Fig. 5(b), where the lowest unoccupied bands around Γ are colored.

The projected density of states (PDOS) for $TlGaS_2$, presented in Fig. 7, is strikingly similar to that of $TlGaSe_2$ in Fig. 4. The bonding character and the origin of bands are the same. The highest occupied bands are related Tl-s orbitals, and the lowest unoccupied bands originate from Tl-p orbitals.

The band dispersions of $TlGaS_2$ in Fig. 6 are reminiscent of $TlGaSe_2$. But, the band gap of $TlGaS_2$ is indirect, unlike

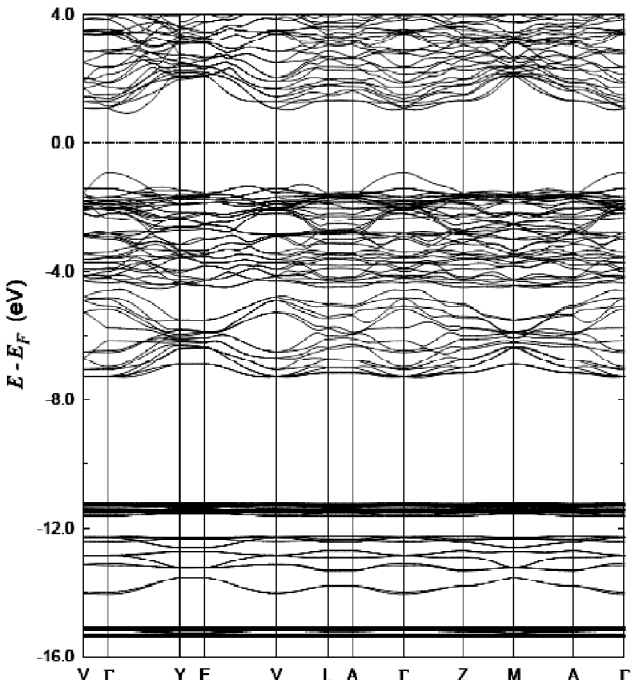

Fig. 6. Electronic band structure of $TlGaS_2$. The energy levels are with respect to the Fermi level E_F.

$TlGaSe_2$. To understand these differences, the electronic structures of $TlGaS_2$ and $TlGaSe_2$ are compared in Fig. 5, where a closer look at the levels near E_F is provided. $TlGaSe_2$ has an additional local minimum on the V-M line, which is not part of the path shown in Fig. 2. The bands that have low dispersion along the V-Γ line are in-layer states. The others have the contribution from the inter-layer Tl-chalcogen interaction. The VBM has a common character for both compounds and, it is closely related to the Tl-chalcogen interlayer interaction. The states involved in CBM are related to Tl-p for both $TlGaS_2$ and $TlGaSe_2$. The bands are slightly mixed for $TlGaSe_2$ while the first unoccupied bands of $TlGaS_2$ in Fig. 5(b) clearly demonstrate the three bands taking part in the CBMs. In Fig. 5(b), Tl-pz orbitals produce a parabolic band, colored red. This red band has Ga-s and S-p antibonding but it has bonding character between the Tl-pz orbitals of adjacent atoms. Therefore, it forms a conduction channel along the Tl chain. These channels are connected along c-axis since the p orbitals of the chalcogens in the adjacent layer appear in the same band. Thus, the red colored band has dispersion along both the V-Γ and the Γ-Y lines. The other two p-orbitals of Tl appear in the blue col-

ored bands, which are flat along the c-axis. Thus, these two bands are related to intra-layer interactions including the Tl-Tl interaction. The red colored band depends on the inter-layer Tl-chalcogen bonds, and the blue colored bands depend on the intra-layer Tl-chalcogen bonds. These three bands produce a single valley in the conduction band of $TlGaS_2$. However, the red colored band shifts down more as a result of the structure relaxation in $TlGaSe_2$. They somewhat mix although the shape of bands is still apparent in Fig. 5(a). As shown in Fig. 5(a), the unequal downshifting results in several valleys in the conduction band of $TlGaSe_2$ with the CBM occurring at Γ.

The CBM is modified by minute changes in the structure even if the inversion symmetry is preserved, explaining the cause of diverse results in the literature[15,24,31,32,34]. There are several valleys in the conduction band of $TlGaSe_2$ with very close minimums. Such valleys are expected to lead to valleytronics[35]. However, the valleys are shallow in $TlGaSe^2$.

$TlInS_2$:

Calculated lattice parameters of $TlInS_2$ in the conventional cell are *a* = 11.192 Å, *b* = 11.197 Å, *c* = 15.225 Å, and β = 100.59°. The lattice constants are bigger by 2% compared to the crystallographic data[36]. The optimized Tl-Tl distance is ≈3.97 Å, and the Tl-Tl-Tl angle is ≈178°, indicating

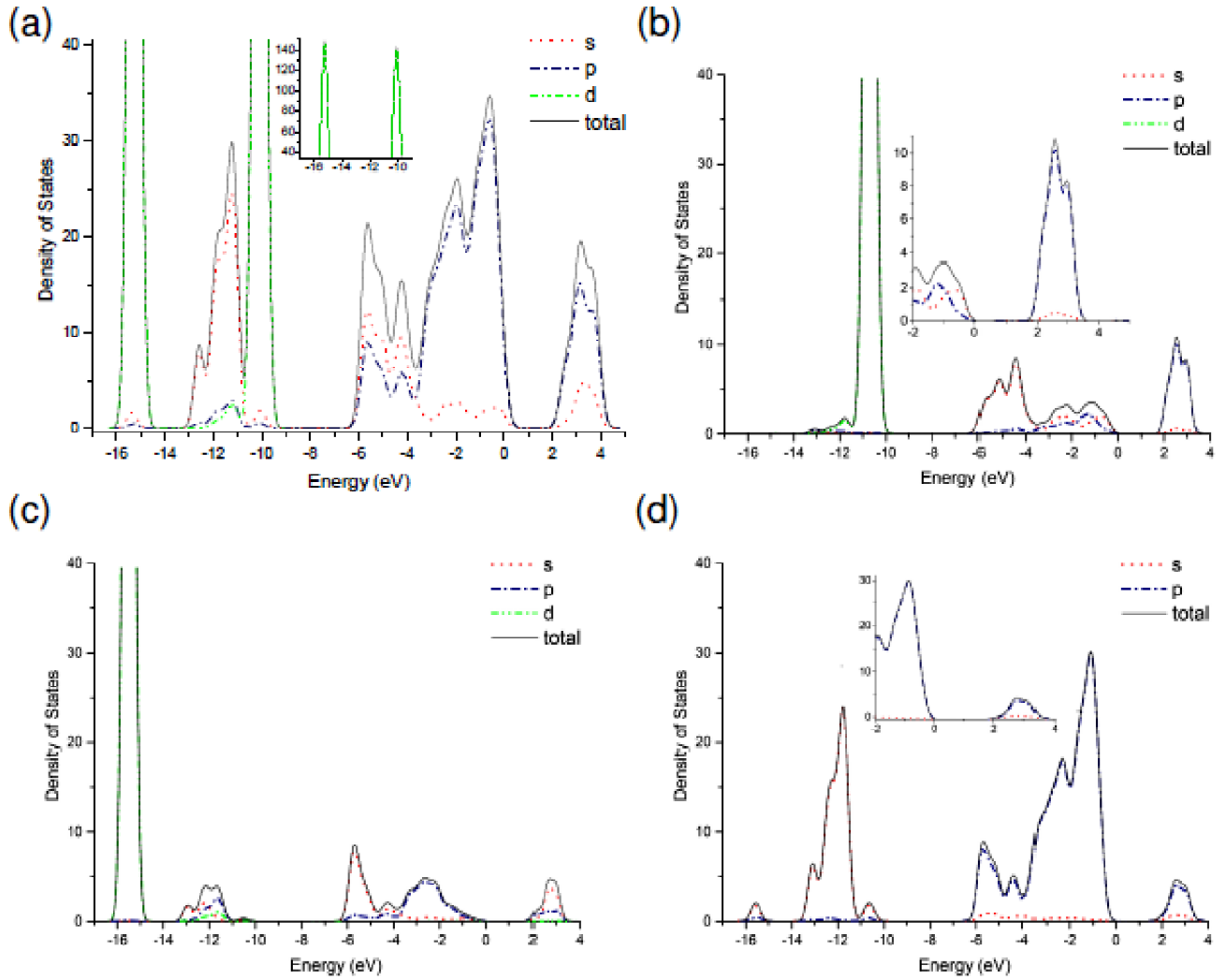

Fig. 7. (a) Electronic density of states (DOS) of $TlGaS_2$ and projected DOS on (b) Tl, (c) Ga and (d) S. The energy is with respect to the valence band maximum (VBM).

almost straight Tl chains. The In-S bond length is ≈2.51 Å, and the Tl-S distance is ≈3.21 Å on the average. The lattice constants *a* and *b* are bigger than $TlGaSe_2$ and $TlGaS_2$ since In has a larger radius than Ga. But, the c value is smaller, indicating a stronger inter-layer interaction. Therefore, the Tl atoms are on a straighter line.

Both the CBM and VBM of $TlInS_2$ is at Γ point in the band structure of $TlInS_2$ presented in Fig. 8. The highest occupied band has the same band shape of $TlGaS_2$, but the unoccupied parabolic band, colored red in Fig. 5(b), shifts down considerably. This band has a contribution from Tl-pz orbitals, and is affected greatly by the inter-layer interaction. The down-shifting is significant in the band structure of $TlInS_2$ because the inter-layer interaction is stronger. We find the direct band gap to be ≈1.5 eV for the optimized structure. The Tl-s orbitals contribute to the highest occupied bands and the Tl-p orbitals contribute to the lowest unoccupied bands. The band characters of $TlInS_2$ are the same as that of $TlGaS_2$. The PDOS plots for $TlInS_2$ are not shown here because they are extremely similar to the results for $TlGaS_2$ shown in Fig. 7. Also in $TlInS_2$, Tl-d orbitals hybridize with the s orbitals of the chalcogen, and thus Tl-S bonds acquire additional directionality. The main source of the directionality in Tl-chalcogen interaction is, of course, the hybridization between the s and p orbitals of Tl. $TlGaSe_2$, $TlGaS_2$, and $TlInS_2$ share the same bonding character but the electronic structures are quantitatively different. Especially, $TlGaSe_2$ has important qualitative distinctions. The VBM is robust in these compounds but the CBM depends heavily on the structural changes, which may be induced by defects or pressure[8,10,25].

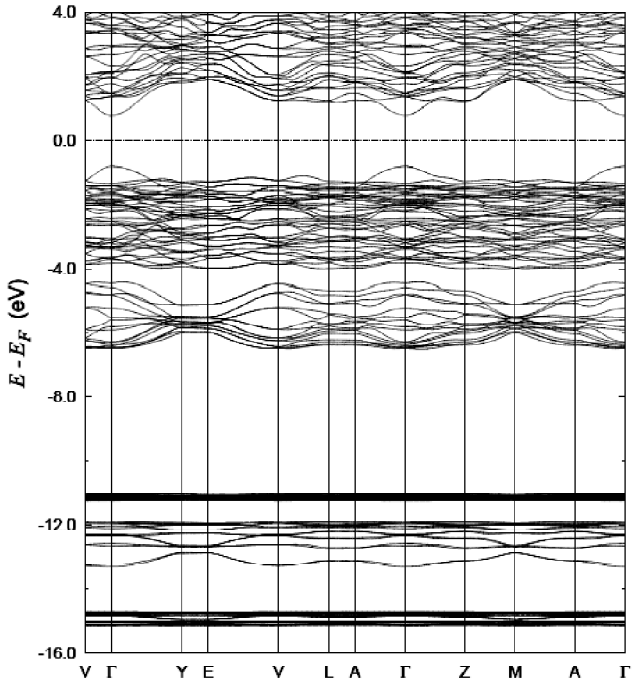

Fig. 8. Electronic band structure of $TlInS_2$. The energy levels are with respect to the Fermi level E_F.

Summary and Conclusions

In summary, we have calculated the electronic structures of isostructural $TlGaSe_2$, $TlGaS_2$, and $TlInS_2$ compounds. The lattice parameter and structure optimizations were performed before the band structure calculations. The calculated lattice constants are within 2% of the experimental values. There are covalent bonds between Ga-S, Ga-Se, and In-S while the Tl atoms weakly bind to the chalcogen. The occupied bands include both bonding and anti-bonding Tl-chalcogen states. The s orbitals of the chalcogen hybridize with the d orbitals of Tl, bringing some directionality to the Tl-chalcogen interaction. The main effect on the directionality is of course due to the hybridization between the s and p orbitals of Tl, interacting with the p orbitals of the chalcogen. There is no direct Tl-Tl bond. The interaction between adjacent Tl atoms is through the Tl-chalcogen bonds. Although the bonding character and the origin of the bands are the same in these three compounds, they exhibit quantitative and qualitative differences. The optimized $TlGaSe_2$ and $TlInS_2$ crystals have direct band gaps while $TlGaS_2$ has an indirect gap. The parabolic unoccupied bands related to Tl-p orbitals play an important role in determining the value and the character of the band gap. The lowest unoccupied states have a bonding character between the p orbitals of the adjacent Tl atoms. These states form conduction channels along the Tl chains. The valence band maximum originates from Tl-s orbitals and its position in the Brillouin zone is robust. The almost degenerate Tl-p related bands are affected differently by the inter-layer interaction. Therefore, minute changes in the structure may shuffle the energy levels, resulting in qualitatively and quantitatively different band gaps in these extremely similar compounds. The band gap of $TlGaSe_2$ changes from indirect to direct after the structure optimization although the changes in the atom positions are not sig-

nificant and the inversion symmetry is preserved. External pressure and defects may initiate the same type of electronic structure changes resulting in unexpected results in experiments. The small amount of down-shifting of the parabolic unoccupied bands leads to several valleys in the band structure of $TlGaSe_2$. Such valleys are essential ingredients of valleytronic. However, the valleys in $TlGaSe_2$ are shallow.

Acknowledgements

Some of the calculations were performed at TUBITAK TRUBA resources.

References

1. D. Muller and H. Hahn, Z. *Anorg. Allg. Chem.* 1978, **438(1)**, 258.
2. W. Henkel, H. D. Hochheimer, C. Carlone, A. Werner, S. Ves and H. G. V. Schnering, *Phys. Rev. B*, 1982, **26**, 3211.
3. A. M. Panich, *J. Phys.: Condens. Matter*, 2008, **20(29)**, 293202/1-42.
4. M. Y. Seyidov and R. A. Suleymanov, *J. Appl. Phys.,* 2010, **108(6)**, 063540.
5. H. D. Hochheimer, E. Gmelin, W. Bauhofer, C. von Schnering-Schwarz, H. G. von Schnering, J. Ihringer and W. Appel, *Z. Phys. B: Condens. Matter*, 1988, **73(2)**, 257.
6. S. S. Babaev, E. Basaran, T. G. Mammadov, F. A. Mikailov, F. M. Salehli, M. Y. Seyidov and R. A. Suleymanov, *J. Phys.: Condens. Matter,* 2005, **17(12)**, 1985.
7. F. A. Mikailov, E. Basaran, L. Tümbek, E. Şentürk and T. G. Mammadov, *J. Non-Cryst. Solids,* 2005, **351(33-36)**, 2809.
8. K. R. Allakhverdiev, T. G. Mamedov, V. V. Panfilov, M. M. Shukyurov and S. I. Subbotin, *Phys. Stat. Sol. (b),* 1985, **131(1)**, K23.
9. S. H. Jabarov, T. G. Mammadov, A. I. Mammadov, S. E. Kichanov, V. B. Aliyeva and E. V. Lukin, *Journal of Surface Investigation,* 2015, **9(1)**, 35.
10. S. Ves, *Phys. Rev. B,* 1989, **40**, 7892.
11. T. G. Mamedov and R. A. Suleimanov, *Phys. Solid State,* 2003, **45(12)**, 2242.
12. K. R. Allakhverdiev, T. G. Mammadov, R. A. Suleymanov and N. Z. Gasanov, *J. Phys.: Condens. Matter,* 2003, **15(8)**, 1291.
13. M. H. Y. Seyidov, R. A. Suleymanov, S. S. Babaev, T. G. Mamedov and G. M. Sharifov, *Phys. Solid State,* 2008, **50(1)**, 108.
14. M. Y. Seyidov, R. A. Suleymanov and Y. Şale, *J. Appl. Phys.,* 2012, **112(10)**, 103106.
15. S. Yang, M. Wu, H. Wang, H. Cai, L. Huang, C. Jiang and S. Tongay, *2D Materials,* 2017, **4(3)**, 035021.
16. S. Johnsen, Z. Liu, J. A. Peters, J. H. Song, S. C. Peter, D. Malliakas, N. K. Cho, H. Jin, A. J. Freeman, B. W. Wessels, *et al., Chem. Mater.,* 2011, **23(12)**, 3120.
17. D. Kahler, N. B. Singh, D. J. Knuteson, B. Wagner, A. Berghmans, S. McLaughlin, M. King, K. Schwartz, D. Suhre and M. Gotlieb, *Nucl. Instrum. Methods: Phys. Res. A,* 2011, **652(1)**, 183.
18. S. G. Abdullaeva and N. T. Mamedov, *Phys. Stat. Sol. (a),* 1986, **133(1)**, 171.
19. K. A. Yee and T. A. Albright, *J. Am. Chem. Soc.*, 1991, **113(17)**, 6474.
20. S. Kashida, Y. Yanadori, Y. Otaki, Y. Seki and A. M. Panich, *Phys. Stat. Sol. (a),* 2006, **203(11)**, 2666.
21. G. Orudzhev, Y. Shim, K. Wakita, N. Mamedov, S. Jafarova and F. Hashimzade, *Jpn. J. Appl. Phys.,* 2008, **47(10S)**, 8182.
22. F. M. Hashimzade, D. A. Huseinova, G. S. Orudzhev, M. A. Nizametdinova, A. M. Ulubey and K. R. Allakhverdiev, *Mater. Res. Bull.,* 2010, **45(10)**, 1438.
23. D. M. Bercha, K. E. Glukhov and M. Sznajder, *Phys. Stat. Sol. (b),* 2011, **248(6)**, 1446.
24. A. Cengiz, Y. M. Chumakov, M. Erdem, Y. Şale, F. A. Mikailzade and M. Y. Seyidov, *Semicond. Sci. Technol.,* 2018, **33(7)**, 075019.
25. M. Y. Seyidov, R. A. Suleymanov and Y. Şale, *J. Phys. Chem. Solids,* 2016, **17**, 96.
26. P. Hohenberg and W. Kohn, *Phys. Rev.,* 1964, **136**, B864.
27. J. P. Perdew, K. Burke and M. Ernzerhof, *Phys. Rev. Lett.,* 1996, **77**, 3865.
28. N. Troullier and J. L. Martins, *Phys. Rev. B,* 1991, **43**, 1993.
29. S. G. Louie, S. Froyen and M. L. Cohen, *Phys. Rev. B,* 1982, **26**, 1738.
30. D. Vanderbilt, *Phys. Rev. B,* 1990, **41**, 7892.
31. M. P. Hanias, A. N. Anagnostopoulos, K. Kambas and J. Spyridelis, *Mater. Res. Bull.,* 1992, **27(1)**, 25.
32. J. A. Kalomiros, N. Kalkan, M. Hanias, A. N. Anagnostopoulos and K. Kambas, *Solid State Commun.,* 1995, **96(8)**, 601.
33. G. E. Delgado, A. J. Mora, F. V. Perez and J. Gonzalez, *Physica B,* 2007, **391(2)**, 385.
34. V. Grivickas, V. Bikbajevas and P. Grivickas, *Phys. Stat. Sol. (b),* 2006, **243(5)**, R31.
35. A. Rycerz, J. Tworzydło and C. W. J. Beenakker, *Nature Phys.,* 2007, **3(3)**, 172.
36. S. Kashida and Y. Kobayashi, *J. Phys.: Condens. Matter*, 1999, **11(4)**, 1027.